NATIONAL ADVISORY COMMITTEE FOR AERONAUTICS

TECHNICAL NOTE 2395

BENCH-TEST INVESTIGATION OF THE TRANSIENT-RESPONSE CHARACTERISTICS OF SEVERAL SIMULATED AIRPLANES INCORPORATING AN AUTOPILOT SENSITIVE TO YAWING ACCELERATIONS

By Donald A. Howard

Langley Aeronautical Laboratory
Langley Field, Va.

Washington
July 1951

NATIONAL ADVISORY COMMITTEE FOR AERONAUTICS

TECHNICAL NOTE 2395

BENCH-TEST INVESTIGATION OF THE TRANSIENT-RESPONSE CHARACTERISTICS OF SEVERAL SIMULATED AIRPLANES INCORPORATING AN AUTOPILOT SENSITIVE TO YAWING ACCELERATIONS

By Donald A. Howard

SUMMARY

An autopilot sensitive to yawing acceleration was used to control four simulated airplane (mass-spring) configurations and a series of bench tests were conducted to determine the response characteristics of the combinations. The occurrence of an unstable mode of motion was predicted in previous theoretical analyses, NACA TN 2006 and TN 2005, in which the autopilot was assumed to have a constant time lag and a constant amplitude ratio. The transient characteristics of the closed-loop system oscillating in yaw were measured and the results show that, with the actual autopilot, no unstable mode of motion was present throughout the frequency range investigated. Examination of the frequency-response characteristics of other existing autopilots indicates that this unstable mode of motion would probably not exist if these autopilots were used, because constant time lag and amplitude ratio do not satisfactorily approximate the frequency-response characteristics of such autopilots in the frequency range where the unstable mode is predicted.

The frequency-response characteristics of the test autopilot were measured separately and were combined with the calculated frequency-response characteristics of the four airplane configurations through use of the method reported in NACA Rep. 882, which was extended to facilitate the determination of the actual transient characteristics of the combined system. The damping and resonant frequency of the system calculated by this method were compared with the damping and resonant frequencies measured from the transient oscillations of the closed-loop airplane-autopilot systems.

INTRODUCTION

At the wing loadings, airspeeds, and altitudes at which present-day airplanes are operating, lateral oscillations with insufficient damping are being encountered. Means have been sought to control these oscillations without necessitating a modification in design which would detract from some desirable feature of the airplane. Rate-sensitive autopilots have been used in some airplanes and have given satisfactory results; however, a rate-sensitive autopilot is limited in satisfactory operation within a certain range of phase angles of lag (less than 90°).

In order to extend the range of phase angles of lag over which satisfactory damping of these oscillations can be obtained, an autopilot sensitive to yawing accelerations was investigated in reference 1. Such a control has the added feature over a rate-sensitive autopilot of not opposing the pilot in steady maneuvers. The results of reference 1, in which the autopilot was considered to have a constant time lag, show that, for a large range of values of time lag, satisfactory damping to the Dutch roll mode can theoretically be supplied by an acceleration-sensitive control; however, in references 1 and 2 a high-frequency unstable mode of motion is predicted to be introduced by the presence of the autopilot. Examination of the frequency-response characteristics of existing autopilots indicates that this unstable mode of motion would probably not exist because the response characteristics determined by use of a constant time lag do not approximate the frequency response of actual autopilots in the frequency range where the unstable mode of motion was found. The constant time lag, however, may satisfactorily approximate the response of a practical autopilot where relatively small phase shifts occur (low frequencies). The analysis, methods, and results obtained in using the concept of constant time lag, therefore, must be carefully qualified and limited in applying results to a practical case.

In order to examine and discuss the limitations of the assumption of a constant time lag, it was considered expedient to obtain quantitative response data not only for an actual acceleration-sensitive autopilot but also for combinations of this autopilot with simulated airplanes for use as examples typical of practical applications. Such measurements were made in the present investigation to obtain the yawing characteristics of four different airplanes that were simulated by a simple mass-spring system.

In addition to these tests the individual frequency-response characteristics of the mass-spring systems were determined and combined with those for the autopilot by the method employed in references 1 and 2 to obtain the degree of stability and natural frequency of the combinations. This method is an extension of the frequency-response method of reference 3 by which the transient characteristics of the combination can be evaluated.

SYMBOLS

δ	servomotor-shaft displacement, radians
ψ	airplane yawing angular displacement, radians
$\ddot{\psi}$	airplane yawing angular acceleration, radians per second per second
ω	circular frequency of oscillation, radians per second
ω_n	natural undamped circular frequency of airplane configuration, radians per second
ω_r	natural damped circular frequency of airplane or airplane-autopilot combination, whichever is applicable, radians per second
N_δ	variation of yawing moment with servomotor-shaft displacement, foot-pounds per radian
I_Z	moment of inertia about vertical principal axis, slug-feet^2
D	differential operator (d/dt)
N_ψ	variation of yawing moment with yawing angular displacement, foot-pounds per radian
N_r	variation of yawing moment with yawing angular velocity, foot-pounds per radian per second
a	real part of complex stability root, $a + i\omega$
γ	logarithmic decrement
$\dot{\psi}$	airplane yawing angular velocity, radians per second
ψ_0	airplane yawing angular displacement at $t = 0$, radians
C_1, C_2	constants
t	time, seconds

APPARATUS

Description of Apparatus

A photograph of the test setup employed in the investigation is shown in figure 1 with the important components of the system labeled.

The automatic pilot used in this investigation employed the rudder amplifier and rudder servomotor of the No. 1 servo-type, P-1 Bendix automatic pilot. In the Bendix automatic pilot, the signals produced by the displacement-gyroscope, rate-gyroscope, and servomotor Autosyns are combined in a mixing unit and transmitted to the servomotor through the amplifier. In order to obtain acceleration signals the displacement-gyroscope and rate-gyroscope Autosyns were replaced by a Statham angular accelerometer. The signal output from the strain-gage circuit of the Statham accelerometer was very low in comparison to the signal output of the Autosyns of the Bendix automatic pilot and, consequently, it was necessary to preamplify the signal. The amount of added amplification was restricted for the following reasons: For a range of low values of acceleration the noise signal produced by the accelerometer masked the acceleration-input signal; additional amplification did not improve the autopilot response characteristics in this region since the noise signal was amplified along with the acceleration-input signal. For the test setup the noise level of the accelerometer was higher than desired partly because of improper energization of the accelerometer bridge circuit. Since it was desired to utilize the source of energization existent in the Bendix automatic pilot, this effect was not corrected. For accelerations above this range of masked response, added amplification of the input signal improved the response characteristics. However, the maximum acceleration signal obtainable was reduced as the amount of amplification was increased because of saturation of the amplifier. Consequently, the amplification was adjusted at a value which enabled the autopilot system to respond satisfactorily at low accelerations just above the noise level and to maintain satisfactory response at relatively large accelerations.

The simulated airplane consisted of a beam free to pivot in yaw about its center point under the restraint of a set of extension springs. The angular accelerometer and a compensating mass were mounted on the beam. The mass characteristics of an airplane were simulated by the mass characteristics of the beam. The springs in the system served to represent the variation of airplane yawing moment with yawing angular displacement and the variation of airplane yawing moment with servomotor-shaft displacement. The model airplane shown mounted on the beam in figure 1 had no significance in relation to the tests but served for demonstration purposes only. The NACA electrical control-position recorders labeled 1 and 2 in figure 1 recorded the motions of the beam

and angular displacement of the servomotor shaft, respectively, on an NACA recording galvanometer. Timing marks of 1/10 second were also recorded.

Operation of Simulated Airplane-Autopilot Combination

When the beam was displaced from a neutral position and released, it performed a damped sinusoidal oscillation in yaw. During this transient motion the system operated as follows: The angular acceleration was picked up by the accelerometer and the signal was amplified in the preamplifier and then mixed in the mixer unit with the negative feedback signal from the servomotor Autosyn so that the static position of the servomotor shaft was approximately proportional to the static input acceleration. The combined signal was then transmitted from the mixer unit through the amplifier to actuate the servomotor. The autopilot response to the sinusoidal oscillation of the airplane, indicated as a servomotor-shaft deflection, was transmitted through a mechanical linkage to produce a yawing moment on the simulated airplane through the rear springs of the system.

METHODS

Measurement of Transient Response of Simulated Airplane-Autopilot Combination

In order to extend the investigation over a range of natural frequencies, four simulated airplanes were tested; each simulated airplane had a specific value of damping in yaw N_r, directional stability N_ψ, and natural frequency. These characteristics of the simulated airplane are a function of the stiffness of the restraining springs shown in figure 1, the moment of inertia of the beam, the internal damping of the springs, and the friction in the beam-pivot bearing. The transient response of each of the configurations to a disturbance in yaw was measured by recording the motions of the beam following its release from a displaced position.

Prediction of Transient-Response Characteristics of Airplane-Autopilot Combination

Reference 3 presents a method for determining whether an airplane-autopilot system is stable or unstable or the existence and frequency of hunting oscillations that may be present in the system by combining the individual frequency-response characteristics of the airplane and autopilot. The predicted transient response presented herein was determined by the methods used in references 1 and 2 wherein the method of reference 3 was extended to include the determination of the degree of stability possessed by the airplane-autopilot combination from the individual frequency-response characteristics of the airplane and autopilot.

Autopilot frequency response.- In figure 2 is shown a photograph of the test setup employed to measure the autopilot frequency response to a constant-amplitude input signal. This system is different from that shown in figure 1 in that the springs were removed, the autopilot servomotor was not connected to the beam, and a direct mechanical linkage was connected from the slide X to the beam to transmit the motions of the slide X to the beam. The slide X was connected eccentrically to a variable-speed, hydraulic transmission and, as a motor drove the transmission, the transmission drove the slide X in approximately sinusoidal motion. The frequency of the oscillation produced was varied by adjusting the rate of fluid flow in the hydraulic transmission. The amplitude of the acceleration at a given frequency was varied by increasing or decreasing the eccentricity of the link connecting the slide X to the transmission. The only function of the simulated airplane and motor-transmission arrangement used in these tests was to feed a sinusoidal oscillation to the angular accelerometer. A block diagram of the system arrangement for measuring the autopilot frequency response is shown in the following sketch:

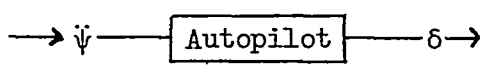

The tests covered a range of yawing accelerations from 0 to 16 radians per second squared and an angular frequency range from 3.0 to 16.7 radians per second (approximately three times the natural frequency of the autopilot). From the galvanometer records of yawing displacement and servomotor-shaft deflection, the phase angle of lag of δ behind $\ddot{\psi}$ as well as the amplitude ratio $\delta/\ddot{\psi}$ were measured as a function of frequency and input amplitude. The angular acceleration was not read directly from the angular accelerometer, but was calculated from the relation $\ddot{\psi} = -\omega^2\psi$. The acceleration was determined in this manner in

order to include the influence of the frequency-response characteristics of the angular accelerometer in the frequency response of the autopilot.

Airplane frequency response.- Since the simulated airplane executes a single-degree-of-freedom motion in yaw, the equation of motion can be written as follows:

$$I_Z\ddot{\psi} - N_r\dot{\psi} - N_\psi\psi = N_\delta\delta$$

or

$$\ddot{\psi} - \frac{N_r}{I_Z}\dot{\psi} - \frac{N_\psi}{I_Z}\psi = \frac{N_\delta\delta}{I_Z}$$

The frequency response of the airplane can be determined directly from this equation provided the coefficients are known. The coefficients were determined as follows:

$$\frac{N_r}{I_Z} = 2a$$

where the value of the quantity a chosen was that value in the relation $\psi_0 e^{at}$ which most closely approximated the rate of decrease of the amplitude of the measured free oscillations of the simulated airplanes. Typical examples of the free oscillations of the four simulated airplanes are shown in figure 3. The coefficient N_ψ/I_Z was determined from the following relations:

$$\frac{N_\psi}{I_Z} = \omega_n^2$$

and

$$\omega_n = \frac{\omega_r}{\sqrt{1 - \frac{\gamma^2}{4\pi^2 + \gamma^2}}}$$

where ω_r is the damped natural frequency of the airplane and was measured from the free oscillation of each of the simulated airplanes. The logarithmic decrement γ was also determined from the free oscillation of each of the simulated airplanes. For all four configurations tested the logarithmic decrement was found to be very small; therefore,

the damped and undamped natural frequencies were very nearly equal. The coefficient N_δ/I_Z was determined from the relation

$$\frac{N_\delta}{I_Z} = \frac{\psi}{\delta}\omega_n^2$$

where ψ/δ was determined by displacing the servomotor shaft and measuring the resulting angle of yaw of the airplane (beam). This quantity is proportional to the yawing acceleration produced by a given servomotor-shaft deflection; any linear one-degree-of-freedom oscillatory system, regardless of size, will perform the same motion for a given servomotor-shaft deflection provided that this quantity and the natural frequency and damping ratio are equal. The values of the coefficients as determined above are listed in table I for the four configurations tested.

The frequency response of the airplane to a sinusoidal input was calculated as follows: Rewriting the equation of motion of the airplane in operator form and rearranging gives

$$\frac{\delta}{D^2\psi} = \frac{D^2 - \frac{N_r}{I_Z}D - \frac{N_\psi}{I_Z}}{\frac{N_\delta}{I_Z}D^2}$$

Substitution of the imaginary frequency $i\omega$ in the preceding relation for the operator D gives the frequency response of the airplane to a constant-amplitude input signal in accordance with the method of reference 3. In the analyses presented in references 1 and 2, the complex quantity $a + i\omega$ was substituted for the operator D. This substitution was also applied in the present analysis and gives the frequency response of the airplane to a damped input signal where the change in amplitude of the input with time is proportional to e^{at}. For each of the four airplane configurations tested, the frequency response was calculated for several values of the damping exponent a.

Airplane-autopilot transient response.- In the method of reference 3 (substitution of $i\omega$ for the differential operator in the equation of motion of the airplane), if a value of frequency can be found for which the amplitude ratios and phase angles of lag of the autopilot and airplane are equal, the combined system will perform a hunting oscillation at that frequency. However, for the extension of this method as used in references 1 and 2 and in the present investigation (substitution of $a + i\omega$ in the equation of motion of the airplane), the values of a and frequency ω for which the amplitude ratio $\delta/D^2\psi$ of the autopilot and

airplane are equal and the phase angle of lag of δ behind $D^2\psi$ of the autopilot and airplane are equal represent the transient characteristics of the airplane-autopilot combination where the transient response is expressed in the form $C_1e^{at}\sin(\omega t + C_2)$. This method is valid provided that the frequency-response characteristics of the autopilot as well as the airplane are obtained subject to damped input signals.

RESULTS AND DISCUSSION

Autopilot Frequency Response

In figure 4 some typical time histories are shown of the autopilot response to a sinusoidal input acceleration as recorded during the measurement of the autopilot frequency-response characteristics. The effects of frequency and acceleration on the autopilot response can be seen from these records. In all test records a pronounced drift in the trim position of the servomotor shaft was indicated. As a result of this drift in trim, the accuracy to which the autopilot amplitude response was obtained was limited and appreciable scatter was evident in the results because of this effect. In figure 5 the amplitude of the servomotor-shaft deflection is plotted against the amplitude of the input yawing acceleration of the simulated airplane for several frequencies. These data were obtained from a series of records like those shown in figure 4. At each frequency investigated, the servomotor-shaft deflection was measured throughout the range of input accelerations available for these tests. The results shown in figure 5 were plotted in this manner in order to be consistent with the method of measuring the results; that is, it was much easier to hold the frequency fixed and vary the acceleration by varying the input amplitude than to fix the acceleration and vary the frequency.

The shaded area at low values of acceleration in figure 5 is a region of questionable response. This region represents the values of input acceleration within which the servomotor deflection did not follow the sinusoidal input acceleration or else followed it intermittently. Because of the erratic response in this range of accelerations, the region could not be defined more precisely.

At each value of frequency tested, a fairing through the experimental data indicated that the amplitude response varied approximately linearly with input yawing acceleration up to a certain value of acceleration above which the output was constant. This limit to the linear response range appeared to be the result of the autopilot saturation. The present investigation was confined to accelerations for which the autopilot had approximately linear response characteristics.

The variation with frequency of the autopilot amplitude ratio δ/ψ and the phase angle of lag of δ behind ψ is presented in figure 6. The data points in this figure are taken directly from the variations shown in figure 5 which are within the range of linear response. The data points exhibit an unusual amount of scatter, and the fairing shown is the theoretical frequency response of a second-order system having a natural frequency of 5.5 radians per second and a damping ratio of 0.3. This fairing agrees reasonably well with the measured data. There are no experimental points in figure 6(a) between frequencies of approximately 5 and 8 radians per second. As a result of the rather rapid decrease of the amplitude ratio in this range of frequencies, the autopilot was quite sensitive to small changes in frequency, and the experimental values of amplitude ratio were somewhat erratic in this frequency range. The phase angle of lag varied from 0° at a frequency of 0 to nearly 180° at the highest frequencies tested and appeared to be approaching 180° asymptotically with increasing frequency. The amplitude ratio dropped off rapidly above a frequency of 5 radians per second.

In several previously reported analyses of the transient characteristics of airplane-autopilot combinations, the frequency response characteristics of the autopilot have been assumed. When assumed response characteristics are used it is necessary that results be qualified in terms of the response characteristics expected from actual autopilots. For example, in references 1 and 2 the autopilot phase angle of lag was represented by the assumption of a constant time lag (a linear variation of phase angle with frequency), and the amplitude ratio was assumed to be independent of frequency (constant). Such assumptions may be justified as representative of many autopilots over a limited frequency range below the primary resonant frequency but, in general, do not apply at higher frequencies. More typical variations through the frequency range are presented in reference 4. As illustrated in reference 4, amplitude ratios may show appreciable variations as resonant frequency is approached and, in general, exhibit considerable attenuation above resonant frequency. The frequency range for a linear variation of phase angle is dependent on the damping in the system and is usually limited to frequencies below primary resonance. At high frequencies the phase angles generally approach a limit as contrasted to the continuous linear increase obtained with the assumption of a constant time lag.

Although the typical frequency-response curves shown in reference 4 apply strictly to a second-order system, examination of experimentally determined frequency-response characteristics of actual autopilots verify the foregoing statements. The magnitude of the phase shifts obtained in practical autopilots may be dependent on the complexity of the system but, since complex systems, which exhibit linear behavior, may be

considered to be made up of second-order (or first-order) systems, the previously described characteristics usually exist.

The assumption of a constant time lag in references 1 and 2 leads to the prediction of a high-frequency unstable oscillation. This condition results because the phase angle of lag of the autopilot servomotor can become greater than 180° and have values in the third and fourth quadrants. Under these conditions a component of the yawing moment applied by the acceleration-sensitive autopilot is in phase with the yawing velocity and results in a reduction in the damping inherent in the airplane. For an autopilot suitable for use as an oscillation damper this unstable mode of motion would probably not exist since the shift in phase angle would be limited. For example, the phase shift for the test autopilot does not exceed 180°, and, consequently, this autopilot would always supply some damping to the airplane.

With regard to the assumption of a constant amplitude ratio, it is evident that the amount of instability contributed by the autopilot at high frequencies as predicted in references 1 and 2 would increase with the magnitude of the amplitude ratio. However, the actual autopilot amplitude ratio rapidly decreased for frequencies higher than the natural frequency (90° phase angle of lag); therefore, even though the phase lag should become larger than 180° at some high frequency, the actual acceleration autopilot should not significantly decrease the damping of the basic airplane because of the small amplitude ratios at high frequencies.

Simulated Airplane-Autopilot Transient Response

Representative time histories of the transient response of each of the airplane-autopilot combinations tested are shown in figure 7. The combinations are numbered in the figure according to the damped natural frequency; that is, the system with the lowest natural frequency is labeled combination 1 and the system with the highest natural frequency is labeled combination 4. The values of the damping exponent a and the natural frequency as measured from the curves are listed in table II for each of the combinations. In all cases investigated the autopilot supplied additional damping to the uncontrolled airplane oscillations and did not produce an unstable high-frequency mode of motion. The increase in damping can be seen by comparing the transient oscillations of the simulated airplanes without the autopilot, as shown in figure 3, with the transient oscillations of the airplanes with the autopilot as shown in figure 7. A comparison of the response of combinations 1 and 2 indicates that the simulated airplane is more highly damped for combination 2 than for combination 1. The reasons for the higher damping of combination 2 are as follows: The phase angle of lag of the servomotor-shaft deflection response behind the angular acceleration of the simulated airplane for combination 2 as compared with combination 1

is much closer to 90° (the phase angle of lag at which the yawing moment supplied by the autopilot produces the maximum opposition to the airplane yawing velocity) and also the yawing moment produced by a unit of servomotor-shaft deflection (N_δ/I_Z in table I) for combination 2 is almost twice the value produced for combination 1. The amount of damping supplied by the autopilot to combination 2 is greater than is evident from comparison of the transient responses of combinations 1 and 2 since the simulated airplane of combination 1 had more inherent damping than that of combination 2 (see values of N_r/I_Z in table I). The relatively poor damping of combinations 3 and 4 as compared with combinations 1 and 2 can be ascribed not only to a difference in phase lags, but also to the large attenuation of the amplitude response of the autopilot at the high natural frequencies of configurations 3 and 4.

The values of the damping exponent a shown for each of the combinations in table II do not represent the maximum damping available for each of the combinations since the damping can be increased by increasing the control effectiveness parameter N_δ/I_Z or by increasing the static sensitivity (amplitude ratio at a frequency of 0), when the autopilot frequency response is assumed to be independent of static sensitivity. The tests were not extended to larger values of a because of mechanical limitations of the system.

The autopilot frequency response to damped input signals was qualitatively investigated from a series of records such as are presented in figure 7 for comparison with the autopilot frequency response obtained from undamped input signals (fig. 4). The assumption was made that the autopilot frequency response to damped input signals as measured from figure 7 was free from any transient components that may have been introduced by the disturbance. The results of this comparison indicate that the phase angle of lag was slightly less in response to damped input signals than in response to undamped input signals. The amplitude ratios $\delta/\ddot{\psi}$ in response to the damped input signals scattered about the faired values obtained in response to undamped input signals.

The limit of autopilot response with regard to small acceleration signals is particularly noticeable as the oscillation amplitude decreases on the servo-deflection traces of combinations 3 and 4 (see fig. 7). At low amplitudes of input signal, the servomotor shaft did not follow the airplane motion. This limit of operation of the autopilot has been discussed previously with relation to figure 4.

In figure 8 the amplitude of the oscillation of airplane-autopilot combination 1 as obtained from a series of records reduced to a common base is plotted and is compared with the relation

$$\psi = \psi_0 e^{at}$$

for various values of the damping exponent a. The damping exponent determines the variation of the amplitude of airplane motion with time. Positive values of the damping exponent indicate divergence of the airplane motion and negative values of the damping exponent indicate convergence. These data indicate that the best fairing through the experimental data is obtained with values of the damping exponent between -0.70 and -0.80.

Results are presented in figure 9 of an investigation of an alternate method for determining the transient characteristics of the test airplane-autopilot combinations. This method was described in the section "Airplane-autopilot transient response" and is illustrated in figure 9 for combination 1. Since the transient response of combination 1, as shown in figures 7 and 8, indicates that the damping exponent a of the system lies between -0.70 and -0.80, the airplane frequency response was calculated by using these values of the damping exponent in the differential equation of motion of the airplane. Because adequate quantitative information was not experimentally obtained on the frequency response of the test autopilot to damped inputs, the autopilot responses presented in figure 9 were calculated for values of the damping exponent of -0.70 and 0 from the same theoretical approximation to the autopilot (second-order equation) employed in fairing the data of figure 6. It would be expected that the airplane and autopilot response curves calculated for a damping exponent of -0.70 would have an intersection of their amplitude ratios at the same frequency as the intersection of their phase angles, a condition which would indicate that the combination of airplane and autopilot would oscillate at this frequency with a damping exponent of -0.70 as measured for this combination. As shown in figure 9, however, the proper amplitude and phase relationships do not exist for a value of the damping exponent of -0.70, and it may be concluded that the assumed second-order equation does not adequately approximate the test autopilot. The intersection criterion is met when the frequency response of the second-order system for the damping exponent equal to 0 is used (see fig. 9), and the same result is also found in the case of the other combinations. The second-order equation did satisfactorily approximate the actual autopilot for the undamped case, and the inference is that the response of the test autopilot to moderately damped input signals does not differ appreciably from the response to undamped input signals. Another phase-angle intersection occurs at a frequency near 4 radians per second (fig. 9) but such intersections are not significant in predicting the actual natural frequency and damping of a system except when accompanied by a corresponding intersection of the amplitude ratios.

CONCLUSIONS

From the results of the tests conducted on an acceleration-sensitive autopilot combined with each of four simulated airplanes, the following conclusions were drawn:

1. An actual autopilot sensitive to angular acceleration did not produce an unstable high-frequency mode of motion of an airplane-autopilot combination. The occurrence of such an unstable mode of motion was predicted in a previous theoretical analysis when the autopilot was assumed to have a constant time lag and a constant amplitude ratio.

2. In the frequency range covered in the tests (from 0 to approximately 3 times the natural frequency of the autopilot), the phase angle of lag of the test autopilot has values such that the autopilot could not produce a decrease in the damping of an airplane.

3. As a result of the rapid decrease of the autopilot amplitude ratio with frequency above its natural frequency, the yawing moments contributed by the autopilot to the airplane at relatively high frequencies with respect to the autopilot natural frequency were small.

4. The assumptions of a constant time lag and amplitude ratio do not satisfactorily approximate the frequency-response characteristics of other existing autopilots at high frequencies. When the concept of constant time lag is used, therefore, care must be exercised in applying results to a practical case.

Langley Aeronautical Laboratory
National Advisory Committee for Aeronautics
Langley Field, Va., September 29, 1950

REFERENCES

1. Beckhardt, Arnold R.: A Theoretical Investigation of the Effect on the Lateral Oscillations of an Airplane of an Automatic Control Sensitive to Yawing Accelerations. NACA TN 2006, 1950.

2. Sternfield, Leonard, and Gates, Ordway B. Jr.: A Theoretical Analysis of the Effect of Time Lag in an Automatic Stabilization System on the Lateral Oscillatory Stability of an Airplane. NACA TN 2005, 1950.

3. Greenberg, Harry: Frequency-Response Method for Determination of Dynamic Stability Characteristics of Airplanes with Automatic Controls. NACA Rep. 882, 1947.

4. Brown, Gordon S., and Campbell, Donald P.: Principles of Servomechanisms. John Wiley & Sons, Inc., 1948, pp. 98-103.

TABLE I

MASS AND AERODYNAMIC CHARACTERISTICS OF THE FOUR AIRPLANE CONFIGURATIONS TESTED

Configuration	N_r/I_Z	N_ψ/I_Z	N_δ/I_Z	ω_n (radians/sec)	I_Z (slug-ft^2)
1	-0.718	-32.6	-5.25	5.71	0.502
2	-.402	-42.0	-9.37	6.48	.502
3	-.440	-88.0	-8.70	9.38	.502
4	-.384	-125.4	-29.80	11.20	.502

NACA

TABLE II

COMPARISON BETWEEN MEASURED AND CALCULATED TRANSIENT-RESPONSE CHARACTERISTICS FOR THE FOUR AIRPLANE-AUTOPILOT COMBINATIONS INVESTIGATED

Combination	a, measured	a, calculated	ω_r, measured (radians/sec)	ω_r, calculated (radians/sec)
1	-0.70	-0.70	5.10	5.56
2	-1.00	-.88	6.42	6.50
3	-.30 to -.40	-.35	9.30	9.30
4	-.30 to -.40	-.30	11.00	12.00

NACA

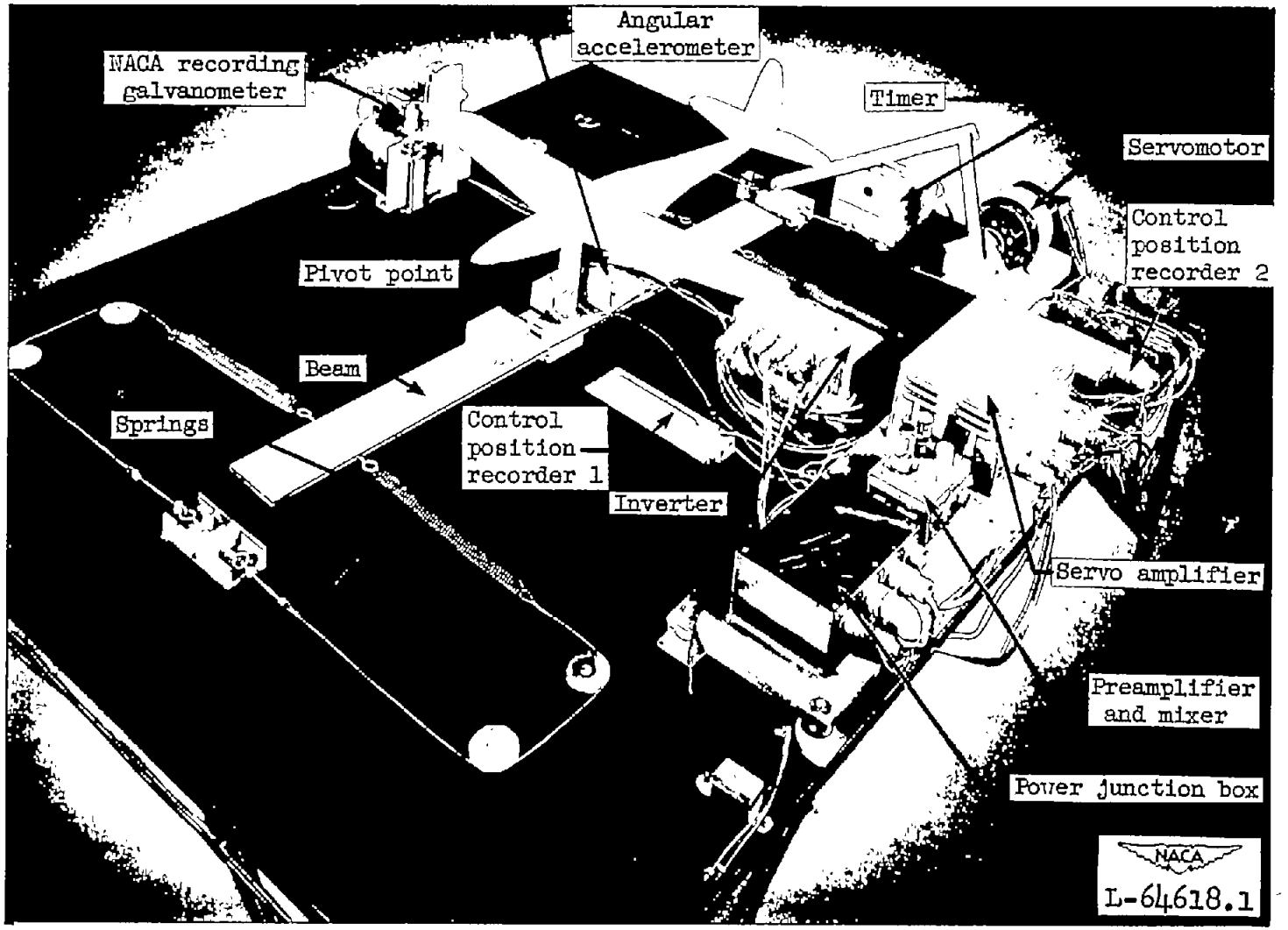

Figure 1.- Bench-test setup for measuring the transient-response characteristics of the closed-loop airplane-autopilot system.

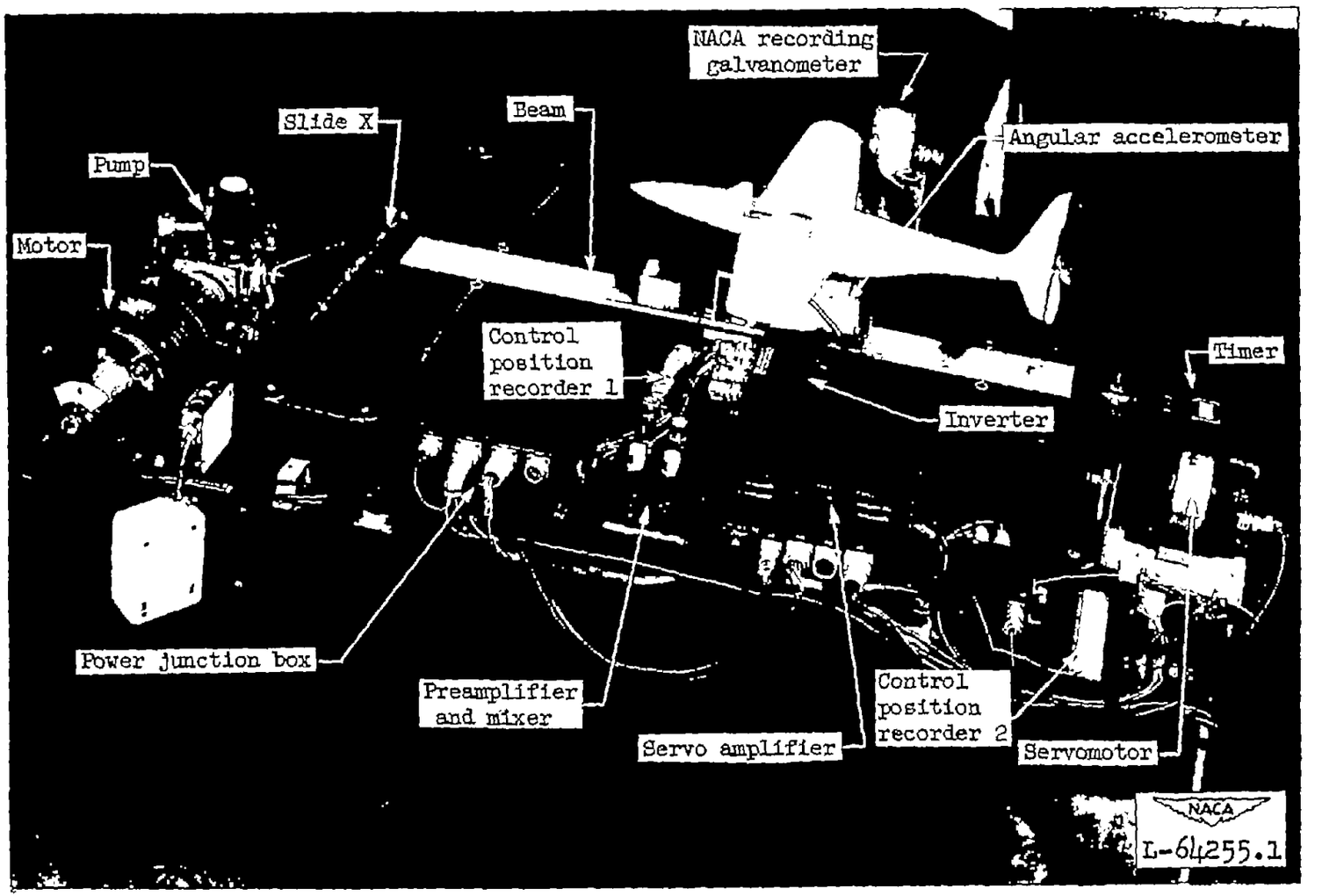

Figure 2.- Bench-test setup for measuring the frequency-response characteristics of the autopilot.

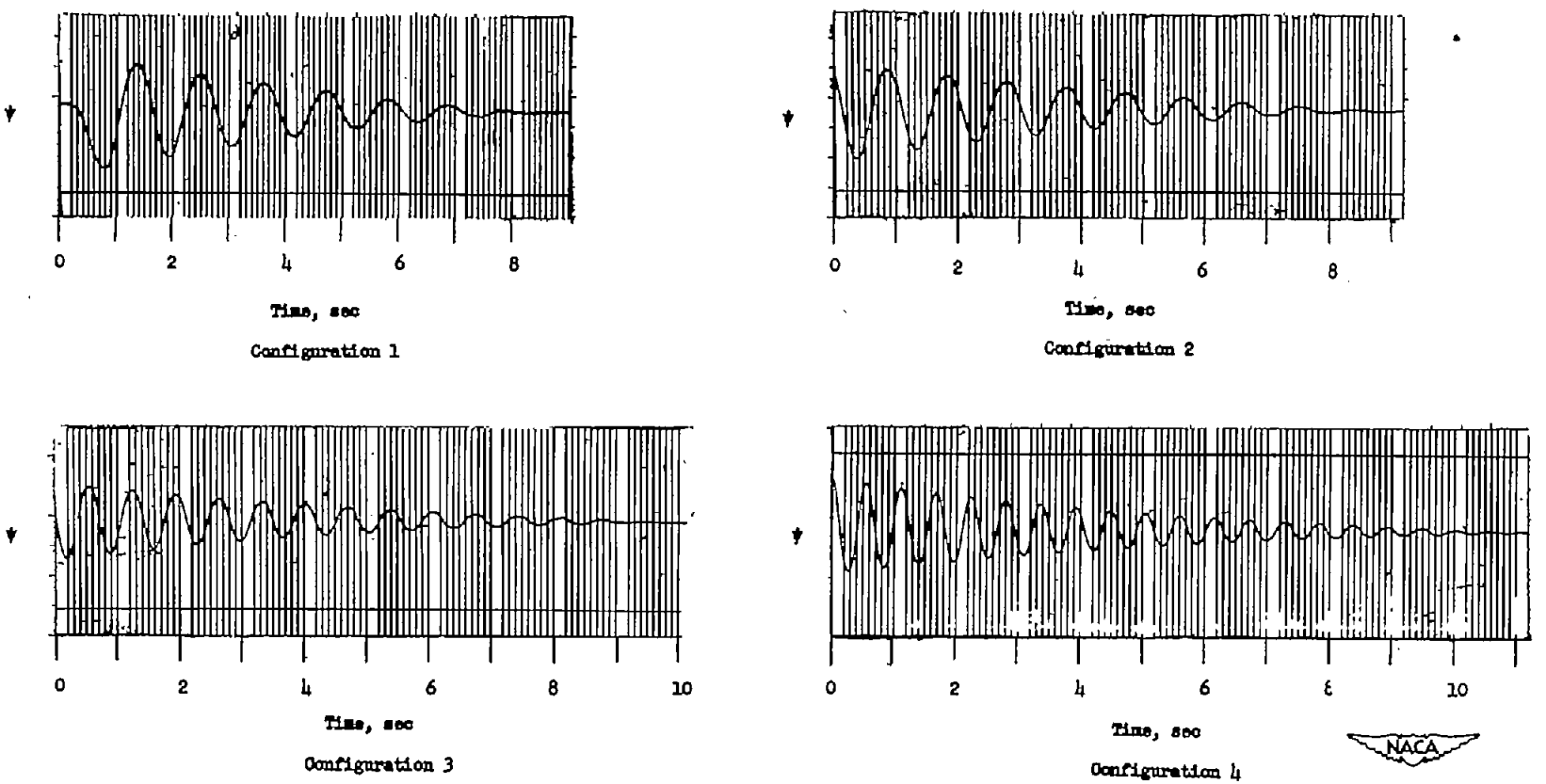

Figure 3.- Typical time histories of the transient response of the airplane configurations, without autopilot, to a disturbance in yaw.

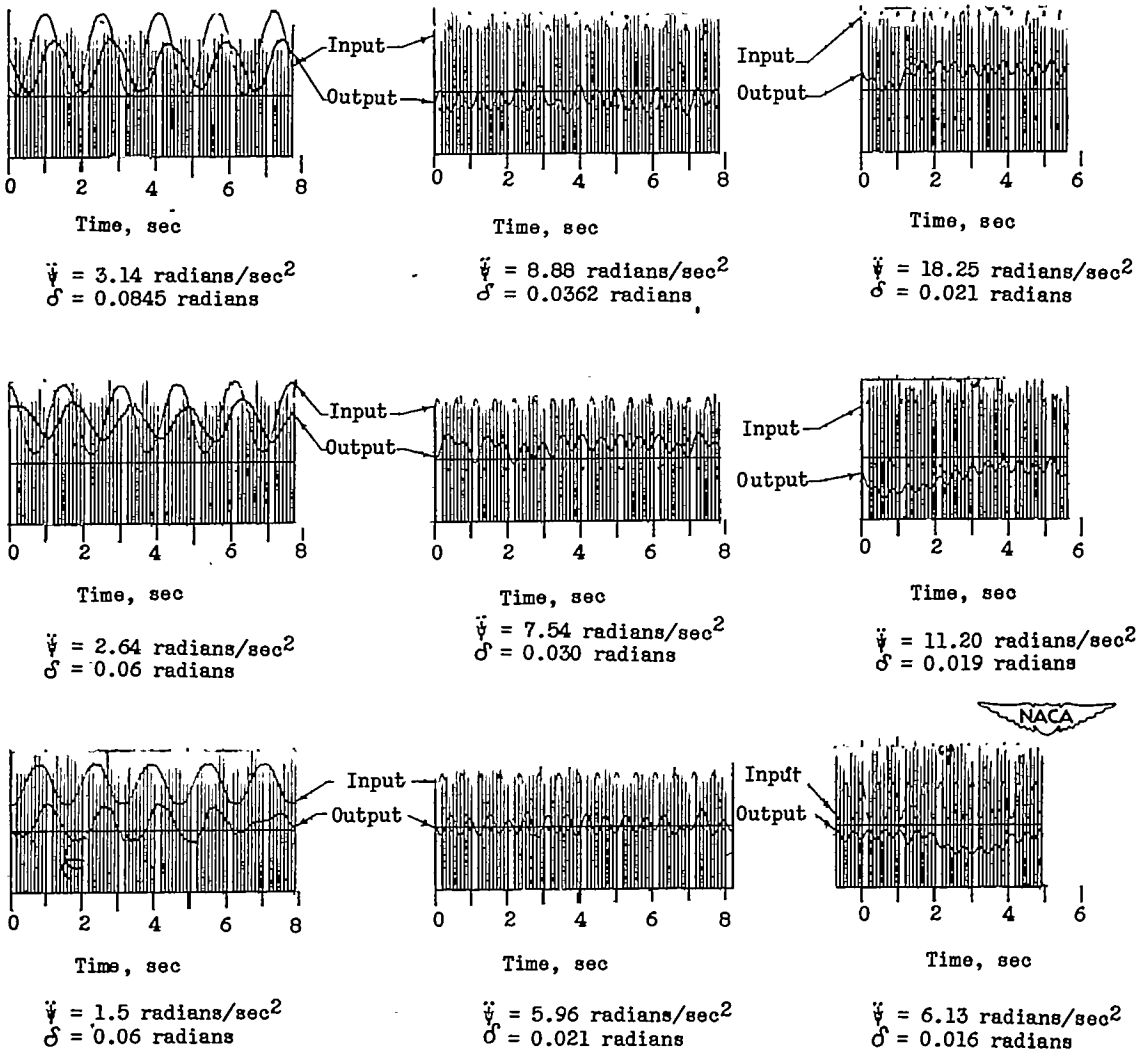

(a) ω = 4.05 radians/sec. (b) ω = 11.64 radians/sec. (c) ω = 14.62 radians/sec.

Figure 4.- Typical time histories of the autopilot response to an undamped sinusoidal input acceleration. Input $\ddot{\psi}$, output δ.

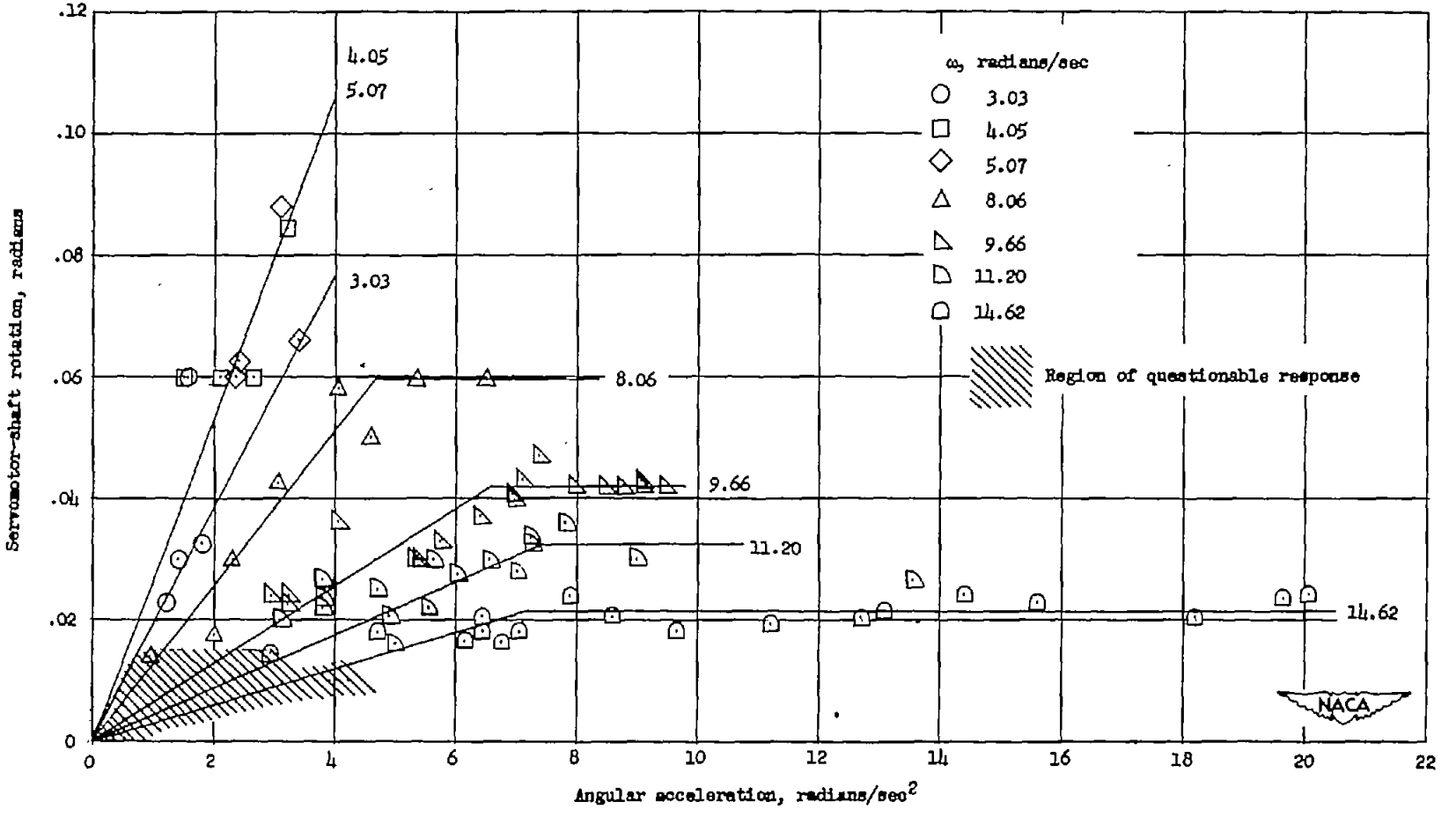

Figure 5.- Variation of the amplitude of the autopilot servomotor response with amplitude of input yawing acceleration for several values of frequency.

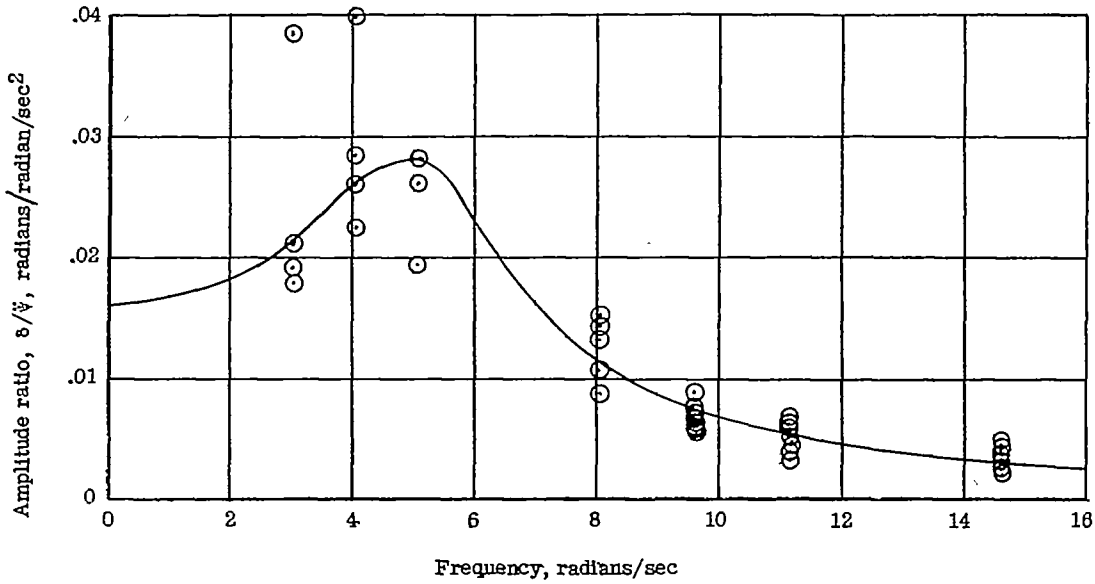

(a) Amplitude ratio, angular acceleration range of 0 to 4 radians/sec.

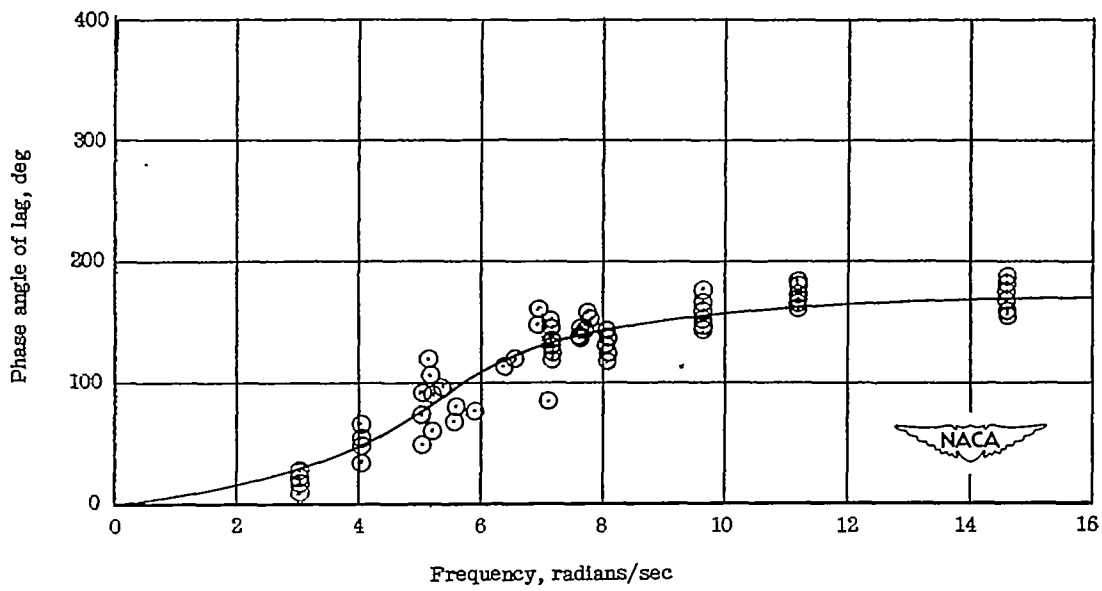

(b) Phase angle of lag.

Figure 6.- Frequency response of test autopilot to undamped input signals. Fairing of test points is second-order equation.

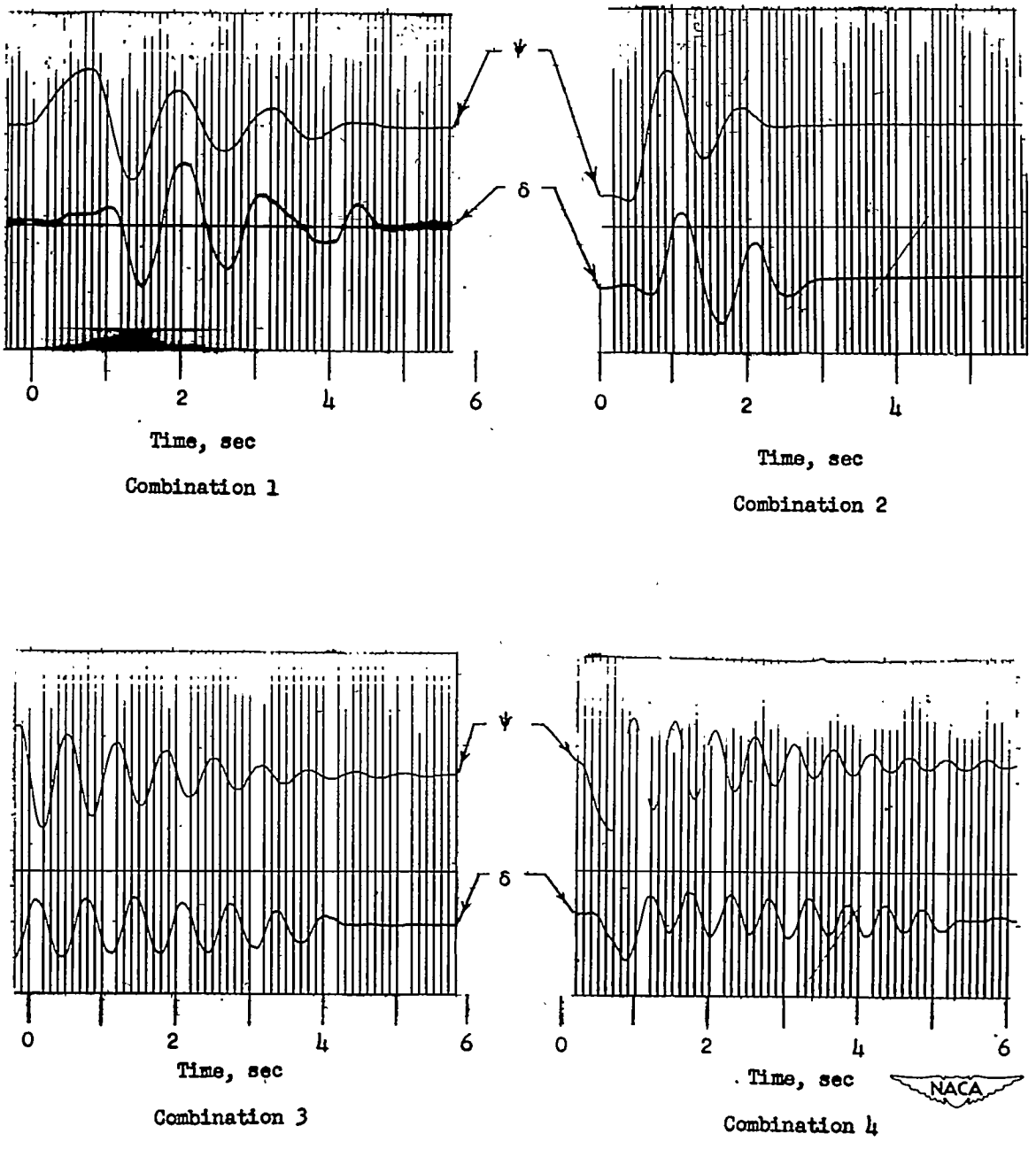

Figure 7.- Typical time histories of the transient response of the airplane-autopilot combinations to a damped disturbance in yaw.

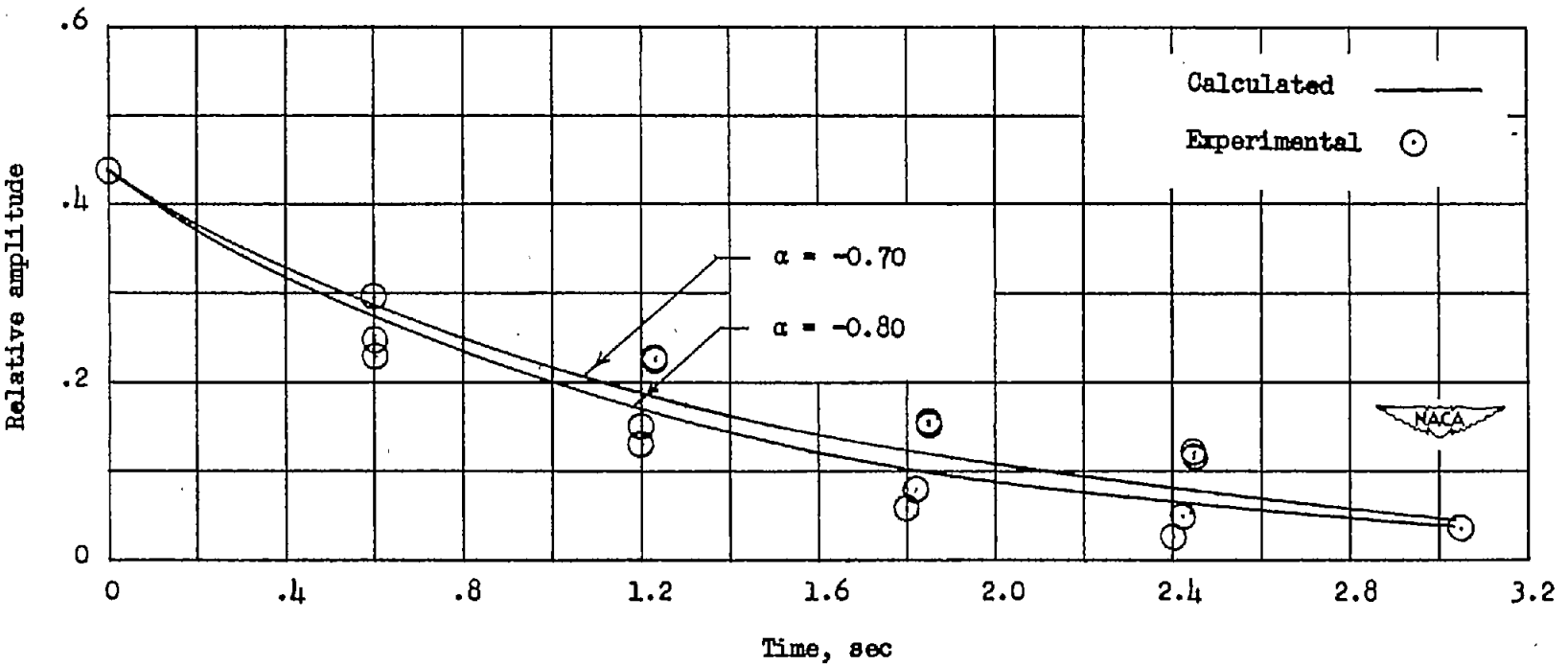

Figure 8.- Variation with time of the amplitude of the transient response of airplane-autopilot combination 1.

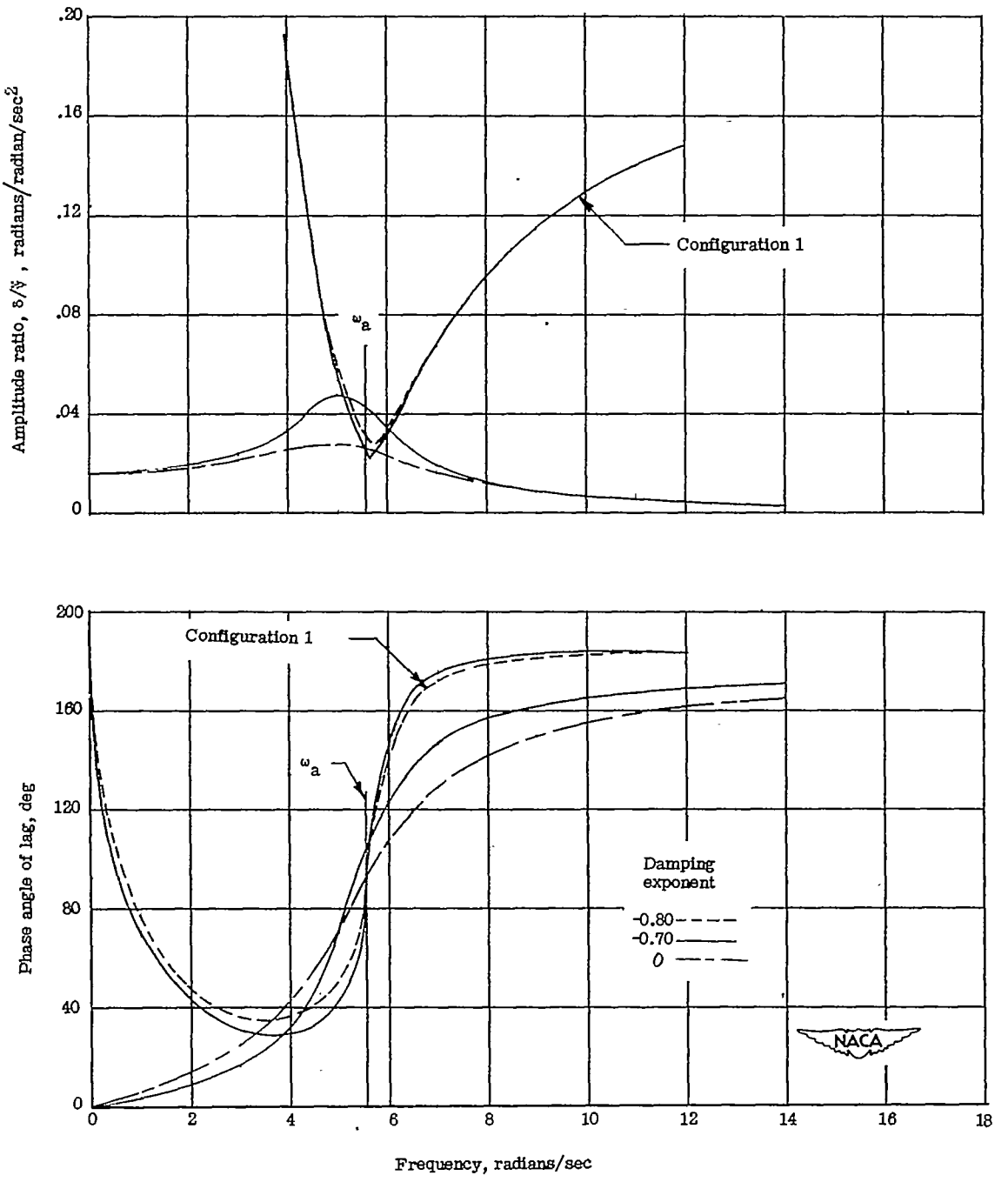

Figure 9.- Frequency response of configuration 1 and of a second-order system approximating the test autopilot. Computations are made for several values of damping exponent.

NACA-Langley - 7-2-51 - 1000